ACS Sustainable Chemistry & Engineering

Research Article

pubs.acs.org/journal/ascecg

Functionalizing Biomaterials to Be an Efficient Proton-Exchange Membrane and Methanol Barrier for DMFCs

Sanna Kotrappanvar Nataraj,*[,†,∥] Chen-Hao Wang,[‡] Hsin-Chih Huang,[§] He-Yun Du,[§] Li-Chyong Chen,[§] and Kuei-Hsien Chen*[,†,§]

[†]Institute of Atomic and Molecular Sciences, Academia Sinica, P.O. Box 23-166, Taipei 10617, Taiwan

[‡]Department of Materials Science and Engineering, National Taiwan University of Science and Technology, Taipei 10607, Taiwan

[§]Center for Condensed Matter Sciences, National Taiwan University, Taipei 10617, Taiwan

[∥]RO-Division, CSIR-Central Salt and Marine Chemicals Research Institute (CSIR-CSMCRI), G. B. Marg, Bhavnagar 364 002, India

Supporting Information

ABSTRACT: Biobased materials capable of transforming into selective proton-exchange composite membranes (PEMs) are highly favored for use in direct methanol fuel cells (DMFCs) because of their low cost and abundance. Here, a polysaccharide and a clay have been functionalized together to make a highly proton selective PEM. Use of chitosan and clay composites ensured limited methanol crossover and thereby high measured performance via efficient fuel convertibility. In this study, sulfonated natural nanocomposite PEMs made of chitosan and sodium−montmorillonite (CS-MMT) were characterized for their water swelling, proton conductivity and methanol permeability parameters. The CS-MMT membrane with a proton conductivity of 4.92×10^{-2} S cm^{-1} and a power density of 45 mW/cm^2 showed a measured methanol crossover current density (J) of <100 mA/cm^2. For higher methanol concentrations (4, 6 and 8 M), fuel loss was ∼4 times less in comparison with commercially successful PEMs, such as Nafion 117.

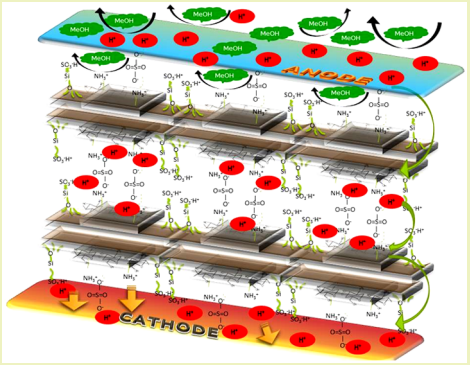

KEYWORDS: *Fuel cell, chitosan, sustainability, proton-exchange membrane, methanol crossover*

INTRODUCTION

With the rapid depletion of fossil fuels and global warming, energy has become the central topic of discussions and plans in the 21st century. This raises the question of an alternative renewable energy source. At present, one of the challenges in overcoming the transition from a carbon based energy source to green energy is to find suitable materials stock. Meanwhile, fuel cells have received widespread recognition as an alternative energy generation technology that is highly efficient and operates in a renewable fuel economy.[1,2] In its own way, direct methanol fuel cells (DMFCs) fulfill the micro-power-supply demand for portable electronic devices, making them one of the best choices among energy sources. Methanol, also known as "wood alcohol", is a renewable energy resource. The high energy density of liquid methanol, no need of a reformer, simple storage, fast refuelling, conventional storage space as well as transport model and low operating temperatures gives DMFCs the potential to outperform other fuel cells.[3−5] Nevertheless, improving the performance and long-term stability are the key factors for success of DMFCs in the market in the near future.

For years, perfluorinated polymer containing sulfonate groups, commercially well-known as Nafion, have been a very successful proton-exchange membrane (PEM) used in DMFCs. However, many studies have pointed out that in the case of DMFCs, a high methanol crossover current density (MCCD) through commercial Nafion series membranes causes substantial fuel loss.[6−8] As a result, poor methanol barrier properties result in methanol flooding at the cathode, reducing the open-circuit potential (OCP) by as much as 0.15−0.2 V and poisoning the electrocatalysts, leading to overall energy loss.[9,10] The main degradation phenomena within membrane−electrode assemblies (MEAs), which directly leads to the measured performance loss, can be categorized in to several processes. MC is among the main reasons that directly imply performance loss in DMFCs. In high methanol concentration operations, significant membrane swelling/thinning occurs, which leads to increased MC and strong mixed potential formation on the cathode.[11]

However, biomaterials are a diverse and versatile class of materials that have potential applications in virtually all sectors of the economy. For the past few years, researchers have spent a considerable amount of time to find the right combination of natural materials for sustainable energy applications. Now, important applications are beginning to emerge in the areas of nanotechnology, biotechnology, packaging, food production

Received: October 30, 2014
Revised: December 29, 2014
Published: January 2, 2015

DOI: 10.1021/sc5005764
ACS Sustainable Chem. Eng. 2015, 3, 302−308

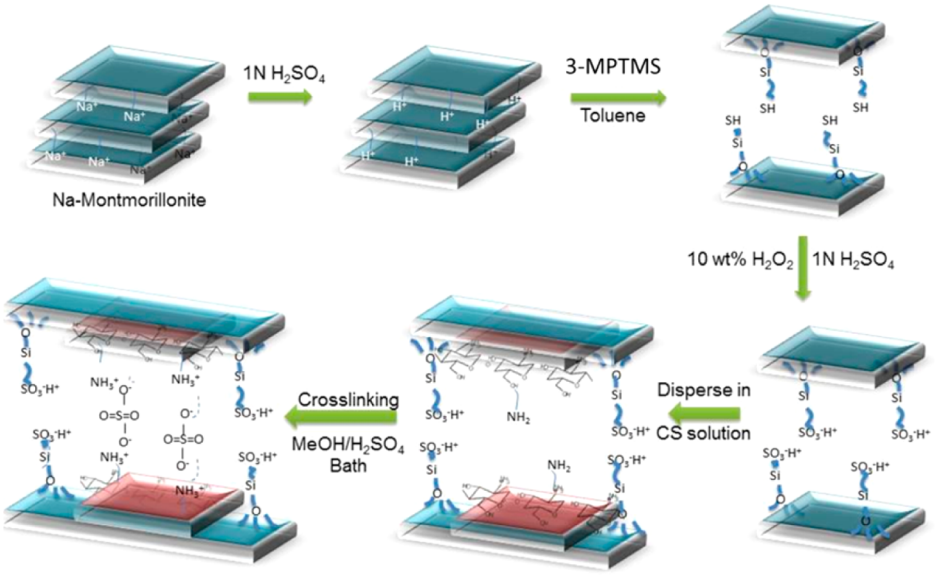

Figure 1. Schematics of functionalizing Na-MMT and CS-MMT membrane by ionic cross-linking with sulfuric acid showing chitosan chain with positively charged $-(NH_3)^+$ and negatively charged sulfuric acid $-(SO_4)^{2-}$ ionic interaction along with sulfonyl functionality of Na-MMT.

and medicine.[12−14] New approaches are being adopted to overcome the limitation of biomaterials in the process of converting them into efficient energy materials. Nevertheless, the difficulties being faced by biomaterials in coming together to make an efficient invention, in many ways, resemble the problems confronting other emerging technologies such as fuel cells.

In an effort to find the right combination of naturally occurring materials, chitosan and clay have been reprocessed in combination with functionalization process to be an efficient PEM in DMFC application. The composites of these materials have been investigated earlier for different characteristics,[15−20] but this study gives a comprehensive overview by engineering a functionalized chitosan−montmorillonite (CS-MMT) into MEAs and evaluates their performances using a fuel cell testing station.

EXPERIMENTAL SECTION

Materials and Membrane Preparation. Chitosan with molecular weight 100 000−300 000 (ACROS Organics, USA), acetic acid, sulfuric acid and methanol were procured from DuPont, USA. Sodium−montmorillonite (Na-MMT) was obtained from Choko Co., Ltd. (Taiwan). A 2 wt % chitosan solution was prepared using acetic acid.

Preparation of Chitosan−Montmorillonite (CS-MMT) Membranes. To functionalize the nanomaterial, Na-MMTs of particle size ∼0.9 μm were first treated with 1 M H_2SO_4 at 25 °C to convert Na^+-MMT to H^+-MMT. Further, the surface functionalization of H^+-MMT was carried out using 3-(mercaptopropyl)trimethoxysilane (MPTMS) at the refluxing temperature of 60 °C in toluene for 24 h. Keeping MPTMS constant, the weight ratio of H^+-MMT and toluene was maintained at 1−10:2:5−20 aiming different end compositions. Prior to sulfonyl functionalization ($-SO_3H$), a thiol ($-SH$) group was grafted onto MMT, which was then oxidized using 10 wt % hydrogen peroxide at 60 °C. The as-prepared sample was then treated with 1 M H_2SO_4 at ambient temperature for complete protonation. Then activated MMTs were washed thoroughly with deionized water and ethanol and dried at 60 °C in a vacuum oven. Finally, sulfonation was carried out using a mixture of 50 mL 1 M H_2SO_4 + 10 mL H_2O_2 under constant stirring conditions for 2 h. To prepare the composite membrane, sulfonated MMTs were dispersed in 2 wt % CS solution with different loadings, namely, 1 wt % (CS-MMT 1), 3 wt % (CS-MMT 3), 5 wt % (CS-MMT 5) and 10 wt % (CS-MMT 10). The composite polymer mixture was hand-casted on a glass plate to prepare the final composite membrane. CS-MMT composite membranes were dried in ambient conditions and peeled from the glass plate. Further, chitosan in composite form was functionalized using a (methanol, 100 mL + H_2SO_4, 3 mL) bath.

Membrane Characterization. The surface morphologies of the pristine CS, cross-linked CS and Na-MMT embedded CS membranes were studied using high-resolution scanning electron microscopy (HR-SEM, JEOL-6700), and the film thickness was directly estimated from the cross-sectional HR-SEM image. Fourier transform infrared-attenuated total reflectance (FTIR-ATR) spectra were obtained by using a PerkinElmer IR (2000) spectrometer (USA) and analyzed with the standard software package, PerkinElmer, Spectrum One. X-ray diffraction (XRD) was carried out using a Bruker D8 advanced diffractometer system with Cu Kα_1 radiation (λ = 0.540 56 Å). The diffractograms were scanned in the range of 0−25° at scan rate of 2° min^{-1}. The basal spacing of the clay was measured according to Bragg's equation: $\sin\theta = n\lambda/2d$.

Water Uptake (%). Water uptake was determined by weighing vacuum-dried membrane and fully equilibrated membrane with water. The surface of the membrane sample was quickly wiped with an absorbent paper to remove the excessive water on the surface, and the sample was then weighed. The water uptake of the membrane was determined as

$$\text{water uptake (\%)} = \frac{W_w - W_d}{W_d} \times 100 \quad (1)$$

where W_w and W_d are the weights of wet and dried membranes, respectively.

Proton Conductivity. Proton conductivity measurements were performed on the membrane using a standard two-electrode cell through ac impedance technique. To measure the proton conductivity of the membrane, membranes were placed between two gold plates, followed by ac impedance measurement (Solartron 1280Z spectrometer) at the frequency range from 20 kHz to 0.1 Hz, with 100% humidity throughout the measurement. The proton conductivity of the membrane can be expressed as

$$\sigma = \frac{L}{R \times A} \quad (2)$$

where R, L and A are the measured resistance, the membrane thickness and the membrane area, respectively.

DOI: 10.1021/sc5005764
ACS Sustainable Chem. Eng. 2015, 3, 302−308

Ion-Exchange Capacity (IEC). The ion exchange capacity (IEC) of the membranes was measured using the classical titration technique. The pretreated membranes in their fully protonated form were immersed in 50 mL of NaCl (2.0 M) solution for 2 h to exchange H^+ in the membrane for Na^+ ions. The solution was titrated with NaOH (0.025 M) to a phenolphthalein end point. Following titration, the membranes were protonated in 0.1 M HCl for 1 h, rinsed with deionized water and dried under vacuum at 80 °C to obtain constant dry weight (m_{dry}). The IEC (mmol·g^{-1}) was calculated from m_{dry}, the volume (V_{NaOH}) and concentration (C_{NaOH}) of NaOH as follows

$$\text{ion exchange capacity (IEC)} = \frac{V_{NaOH}C_{NaOH}}{m_{dry}} \quad (3)$$

Membrane–Electrode Assembly Fabrication and Tests. The membrane–electrode assembly (MEA) is a sandwiched structure, where the membrane is sandwiched between the anode and the cathode. In the preparation of the MEAs, electrodes of a 80 wt % 4.0 mg·cm^{-2} Pt–Ru on carbon cloth and a 5.0 mg cm^{-2} Pt black on carbon cloth were used as the anode and cathode, respectively. They underwent the same hot-pressed condition at 130 °C and 130 kg·cm^{-2} for 2 min. To understand MEA performances under various methanol concentrations, 2, 4, 6 and 8 M methanol solutions were pumped into the anode chamber at a rate of 20 mL·cm^{-3} and the oxygen flowed into the cathode chamber at a rate of 200 sccm. The cell temperature was maintained at 60 °C during all the measurements.

The methanol-crossover rate of MEA was determined by an electrochemical technique mentioned in a previous study.[21] The nitrogen flowed into the cathode at a rate of 200 sccm, and a positive voltage was applied to the cathode using a potentiostat (SI 1280Z, Solartron). Therefore, the methanol at the cathode was oxidized to CO_2 under the applied voltage. When the applied voltage was high enough to oxidize all methanol molecules quickly at the cathode, the methanol-crossover limiting current was reached, which was associated with the methanol-crossover rate at the open circuit.[22]

RESULTS AND DISCUSSIONS

Characterization of the Natural Composite Membranes. The preparation steps of natural nanocomposite PEMs have been systematically investigated. First, Na-MMT was sulfonated in a separate step using H_2SO_4 and MPTMS followed by H_2O_2/H_2SO_4 bathing, as depicted in a schematic illustration in Figure 1. To prepare membranes, sulfonated clay (S-MMT) was dispersed in 2 wt % chitosan solution and sonicated for an agglomeration free solution. Different loading percentages of composite solutions were cast on a glass plate and dried in ambient conditions. Prior to single unit cell preparation, membranes were post-treated using a mixture of H_2O_2+H_2SO_4 bath. The reaction process was monitored by analyzing samples at each step by XRD and FTIR. The CS-MMT composite membranes were also characterized by various physical and chemical techniques.

To confirm the sulfonation on Na-MMT, small angle XRD was performed on Na-MMT and functionalized ordered nanoporous MMT. XRD measurement is a powerful tool to understand the changes in the structure of the clay environment, because the interlayer can be estimated by the measuring the d_{001} spacing. Figure S1 (Supporting Information) shows the XRD patterns of starting Na-MMT and sulfonated-MMT in the form of dry mass. The characteristic peak of Na-MMT (Figure 3a,a1) at a diffraction angle of $2\theta = 6.2°$, corresponding to the basal spacing of 1.45 nm shifted to $\sim 2\theta = 2.3°$ in the sulfonated sample, as shown in Figure S1b (Supporting Information) and schematically illustrated in Figure S1b1 (Supporting Information). The absence of this peak is due to the exfoliated structure formed by too large of spacing between the layers. The increase of basal spacing indicates that MMT layers were well intercalated by the sulfonic acid groups.

The compositions of the CS-MMT membranes before and after functionalization have been analyzed by using ATR-FTIR spectroscopy. In Figure S2c (Supporting Information), the characteristic Si–O–Si stretching vibration band of the MMT upon MPTMS treatment occurs at ~1070 cm^{-1}, 1080–1106 cm^{-1} ν_δ SO_3^- overlapping and 500–600 cm^{-1} deformation of O–H groups linked to the interlayer cations. This fact can be related to the electrostatic interaction between SO_3^- groups and the negatively charged sites in the clay structure.

Chitosan, with a high chelating ability, in combination with its high percentage of nitrogen present in the form of amine groups, is responsible for ion exchange mechanism in acidic media. Amine sites are the main reactive groups, which readily undergo a protonation process. An elaborated analytical trend of CS and intercalation of sulfonated MMT is shown in Figure 2a. In addition, the vibrational band characteristics of the S-MMT at 3635 cm^{-1}, υOH of H_2O ≈ 3430 cm^{-1}, δHOH ≈ 1640 cm^{-1} and υSiO of Si–O–Si ≈ 1050 cm^{-1}, the bands attributed to the intercalated chitosan are also observed in the spectra of the nanocomposite. The frequency of vibrational

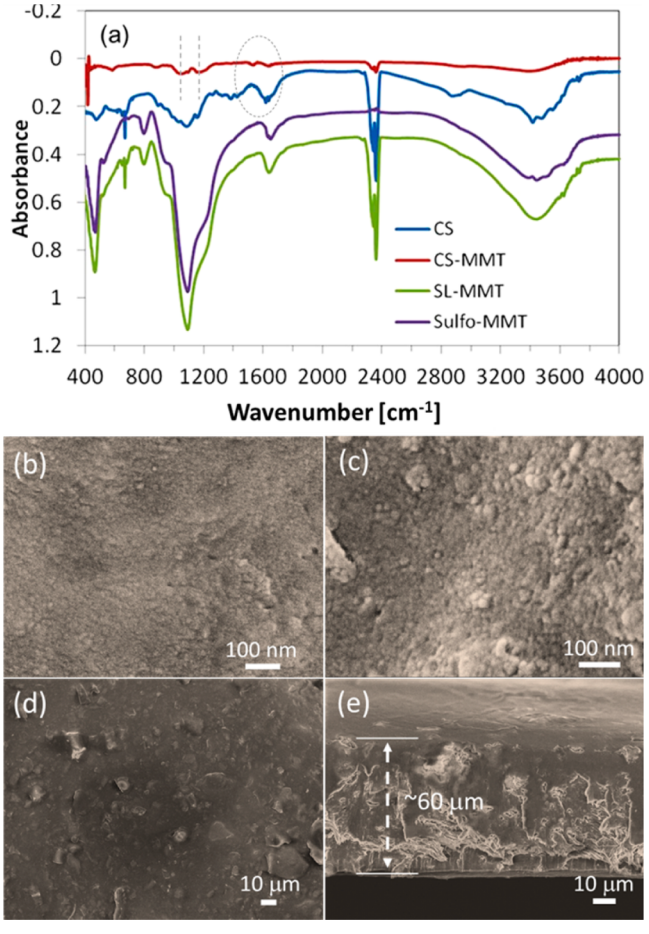

Figure 2. (a) ATR-FTIR of CS-MMT natural nanocomposite membrane intercalation process by FTIR monitoring. Spectra covers CS, CS-MMT control samples and sulfonated MMT (S-MMT) and S-MMT in CS matrix. All samples were of 3 wt % MMT loading taken as the optimized condition. HR-SEM images to characterize surface morphologies of (b) CS-MMT 1%, (c) CS-MMT 3%, (d) CS-MMT 10, and (e) cross-sectional view of CS-MMT 3% with thickness of ~60 μm.

DOI: 10.1021/sc5005764
ACS Sustainable Chem. Eng. 2015, 3, 302–308

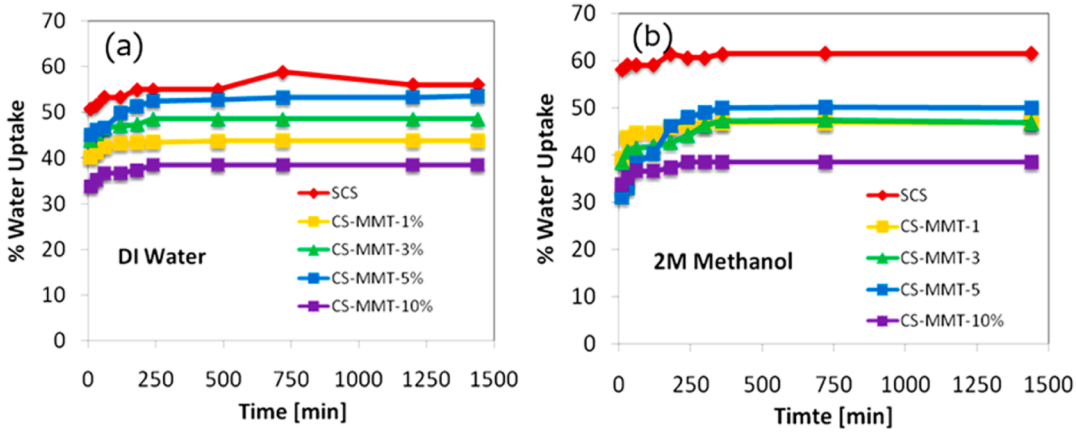

Figure 3. Water uptake properties of cross-linked chitosan and different S-MMT weight loaded chitosan membranes in (a) DI water and (b) 2 M methanol solutions performed at room temperature (25 °C).

bands at 1560 cm^{-1} in the starting chitosan, which corresponds to the deformation vibration ($v\delta_{NH3}$) of the protonated amine group, is shifted toward a lower frequency value, whereas the marked area in Figure 2a identifies symmetrical stretching of $-SO_2N-$ at 1143 cm^{-1}; SO_3^- symmetric stretching around 1057 cm^{-1} confirms the strong interaction between modified clay and the polymer. This can be attributed to the electrostatic interaction between sulfonyl groups and the negatively charged sites in the clay structure. The vibrational bands in the starting chitosan υ_{CO} of C−O−C ∼ 1075 cm^{-1} characteristic of the piranose ring and υ_{OH} ∼ 3356 cm^{-1} overlap with the bands of the MMT. In the case of the nanocomposite prepared from the CS-MMT 3 wt %, the band at 1721 cm^{-1} may be assigned to the υCO stretching band of acetate ions associated with the second layer of chitosan (Figure 1). In addition to this, the broad band at $\tilde{\nu}$ = 1150−1100 cm^{-1}, which has been assigned to C−N, and the band at $\tilde{\nu}$ = 3400 cm^{-1}, which is associated with O−H stretching from CS-MMT, confirm the sulfonic acid functionalization on composite membrane. Upon cross-linking, additional hydrogen bonding and the dense nature contributed to higher mechanical performances of the membrane during MEAs hot press occurs.

The HR-SEM images show the good dispersion for low loadings of MMT in the CS matrix. The SEM images of various compositions display clearly a smooth surface with uniformly dispersed sulfonated MMTs with low percent of loadings. At a lower MMT loading up to 3 wt %, the MMT shows the coexistence of the CS- and S-MMT phases with good interfacial contact. Large clusters or aggregates of S-MMT particles were not visible in SEM images. Figure 2b,c gives CS-MMT loadings of 1 and 3 wt %, respectively. With the increased amount of S-MMT (5−10 wt %), the membrane became rigid and the dispersion of sulfonated MMT aggregated more like flakes in the dried membrane, which is clearly visible in Figure 2d. It was also observed higher loading of S-MMTs island-like clusters in the polymer matrix, which consequently induces a poor polymer−MMT interface. To confirm the bulk microstructure, CS-MMT 3 wt % was examined with cross-sectional morphology. Throughout the thickness of ∼60 μm, CS continuous phase shown miscibility with sulfonated MMT nanoparticles.

The proton conductivity and methanol permeability factors strongly depend on water uptake (WU) properties of the material. An adequate level of water uptake is essential to maintain good proton conductivity. However, water uptake ought to be minimized or controlled to ensure membrane swelling, thereby ensuring low methanol permeability. The trends in the %WU of the pristine cross-linked CS and MMT embedded CS in DI water and 2 M methanol are shown in Figure 3a,b, respectively. The WU characteristics of the CS composite membranes are mainly governed by the hydrophilic characteristics of the chitosan ionomer, and sulfonation cross-linking plays a dominant role in controlling WU. It is interesting to note that WU, as a whole, is independent of methanol concentrations recorded. The average %WU for SCS (58%), CS-MMT 1% (43%), CS-MMT 3% (45%), CS-MMT 5% (48%) and CS-MMT 10% falls to (35%) in DI water and 2 M methanol solution.

The PEM is a polymer network containing covalently bonded negatively charged functional groups capable of exchanging cations. For FCs, the sulfonic acid group ($-SO_3^-$) is the widely used exchanging site because the protons are fully dissociated in the presence of water, thereby functioning as a good hydronium ion conductor.[23] Utilizing WU data, we determined the ion-exchange capacity of the CS-MMT membrane along with that of the control and Nafion as a reference. Comparative IEC and proton conductivity data is presented in Table 1. Enhanced IEC in CS-MMT is attributed to the presence of excessive sulfonyl active sites from S-MMTs in ionically cross-linked chitosan. This may lead to selective transport of protons across the membrane through interconnected hydrated domains. On the other hand, proton conductivities for CS-MMT membranes are moderate and show an increasing trend up to an optimized 5% embedded

Table 1. Physicochemical Properties of Na-MMT, S-MMT, CS- and S-MMT Intercalated CS Membranes in 2 M Methanol

membrane (mmol·g^{-1})	proton conductivity (S·cm^{-1})	ion-exchange capacity
Na-MMT		0.49
sulfonated MMT		2.08
cross-linked CS	0.006	1.01
CS-MMT-1%	0.0342	2.30
CS-MMT-3%	0.0486	2.73
CS-MMT-5%	0.0492	2.21
CS-MMT-10%	0.0263	1.90
Nafion 117	0.098	0.95

DOI: 10.1021/sc5005764
ACS Sustainable Chem. Eng. 2015, 3, 302−308

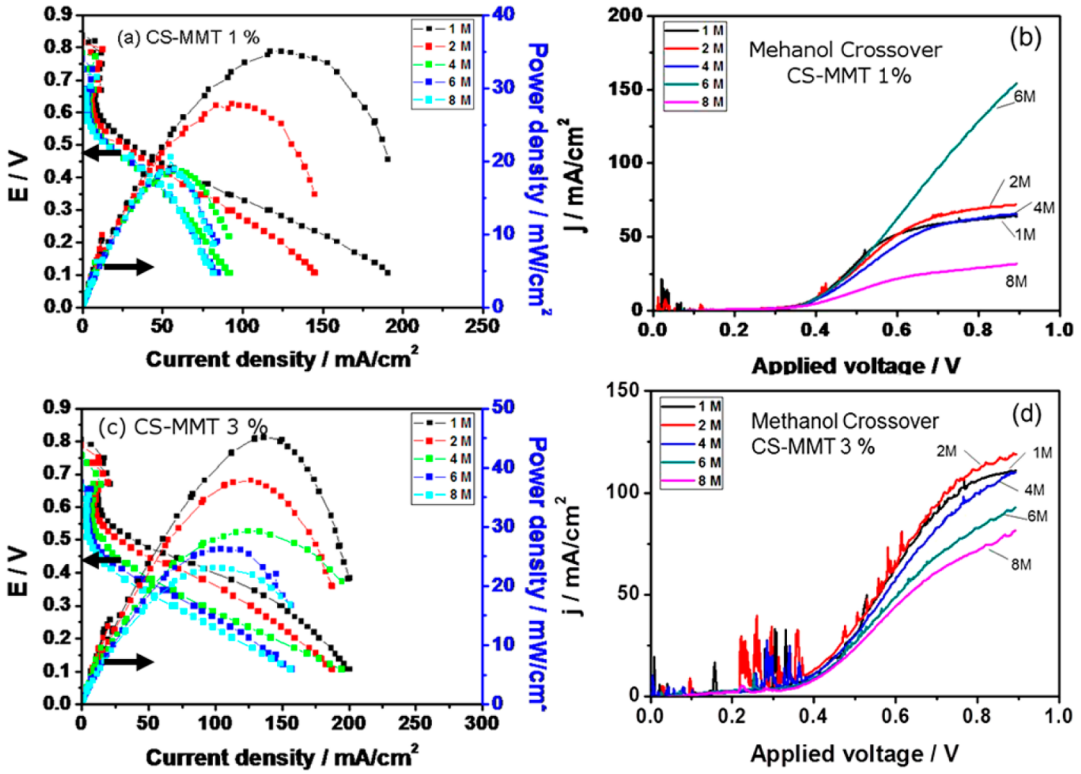

Figure 4. (a) Polarization curves of CS-MMT 1% and (b) its MCCD measurements as a function of applied voltage. (c) Polarization curves of CS-MMT 3% and (b) its MCCD measurements (MEA operated at various methanol concentrations; oxygen flow rate of 200 sccm, methanol flow rate of 20 mL min^{-1} and cell temperature of 60 °C).

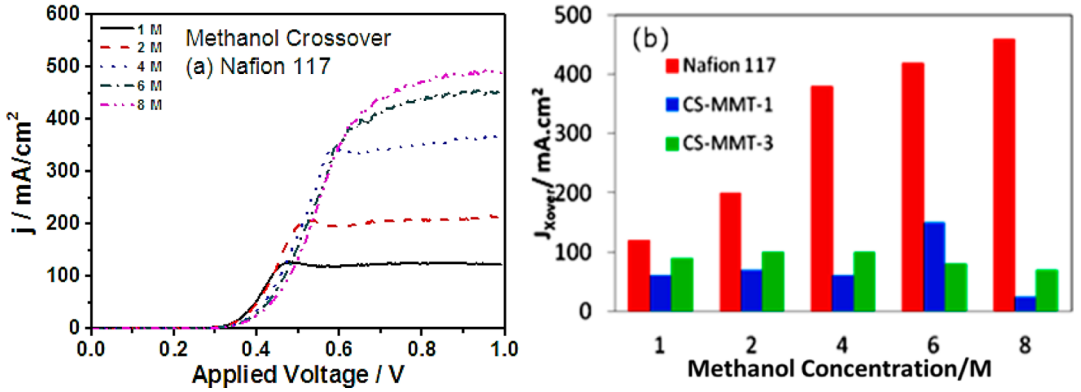

Figure 5. (a) Comparative measurement of methanol crossover current density as a function of applied voltage for commercial standard PEM-Nafion 117 and (b) comparative representation of methanol-crossover limiting current densities determined by the applied voltage of 1 V that of CS-MMT 1% and CS-MMT 3% with different methanol concentrations.

sulfonated MMT. The proton conductivity increased until an optimal 3% MMT loading, which corresponds to an increase in IEC. Higher loading MMT over 3% resulted in aggregate formation, leading to uneven distribution in the parent CS matrix. The proton conductivity for as-prepared membranes ranged between 4.92×10^{-2} S cm^{-1} (CS-MMT 5%) and 2.63×10^{-2} S cm^{-1} (CS-MMT 10%), which is closer to the pristine commercial 9.8×10^{-2} S cm^{-1} (Nafion-117) membrane. However, higher proton transportation in Nafion 117 is attributed to well-connected channels formed by ionic clusters of hydrophilic sulfonic groups, whereas the higher IEC in CS-MMT 3% membrane (2.73 mmol·g^{-1}), in comparison to that of Nafion 117 (0.95 mmol·g^{-1}), suggests the formation of a network of active sulfonyl sites. This eventually leads to enhanced proton propagation. It was apparent that the higher cross-linking density and loading in CS-MMT decreases the proton conductivity as well as IEC, resulting in a rigid chitosan matrix.

MEA Performance. Figure 4 shows the I–V polarization curves and power density curves at recorded at different methanol feed concentrations. To quantify the MEA performances under various methanol concentrations (1, 2, 4, 6 and 8 M), solutions were pumped into the anode chamber at a rate of 20 mL·cm^{-3} and the oxygen flowed into the cathode chamber at a rate of 200 sccm. The cell temperature was maintained at 60 °C for all the measurements. Open-circuit potential (OCP) and power densities reach an almost steady-state for all concentrations of the methanol feed. I–V curves (Figure 4a,c)

DOI: 10.1021/sc5005764
ACS Sustainable Chem. Eng. 2015, 3, 302–308

Table 2. Comparative Methanol Crossover Current Densities for Different Membranes in DMFC

membrane	MLCD (J_{xover}) mA/cm^2	methanol concentration (M)	reference
Nafion 212 at 55 °C	358	6	26
Nafion/SiO_2/m-BOT at 55 °C	285	6	26
sulfonated PEEK	70−120	1	27
Pd−Nafion	100−400	1, 2, 5	28
PBI-PVPA	50−120	1, 3, 4	29
diphenylsilicate−Nafion	160−183	1, 4, 10	30
polyaniline−Nafion	50−300	1, 2, 4, 6, 8	31
Nafion 117	120−480	1, 2, 4, 6, 8	31
chitosan−Nafion	100−225	2, 4, 6, 8	32
CS-MMT	27−110	1, 2, 4, 6, 8	present study

show reasonable single cell behavior for CS-MMT 1 wt % and CS-MMT 3 wt %, reaching power densities up to 45 mW/cm^2, very close to those recorded for the commercial copolymer Nafion in the same conditions (~52 mW/cm^2). The power densities have shown higher stability as a result of enhanced selectivity at higher methanol concentration feeds (4, 6 and 8 M), which was recorded to be ~30 mW/cm^2 for the CS-MMT 3 wt % natural nanocomposite.

Stable performance of a membrane in higher methanol concentration operations is crucial for efficient single cell output. Limiting the methanol crossover to the cathode prevents flooding, thereby retaining the sensitivity of the cathode. To measure the membrane fuel efficiency, crossover limiting current density was measured as a function of applied voltage at different methanol concentration, as shown in Figure 5b,d. Accordingly, limiting current densities for CS-MMT 1 wt % and CS-MMT 3 wt % were <110 and ~100 mA/cm^2, respectively, whereas that of reference membrane Nafion 117, tested at similar conditions, ranged between 110 and 480 mA/cm^2 for methanol concentrations of 1 to 8 M solutions, as shown in Figure 5a. A maximum value of ~110 mA/cm^2 for CS-MMT membranes at higher concentrations indicates improved selectivity toward protons. Figure 5b gives a comparative representation of MCLC densities for CS-MMT membranes in comparison with Nafion 117 estimated at the applied voltage of 1 V. Even though an unusual rise was seen in 6 M for CS-MMT 1 (~150 mA/cm^{-2}). which may be attributed to excessive swelling of membrane under given testing conditions, an overall ~3-fold reduction in methanol crossover was recorded for CS-MMT membranes. Methanol permeates through the membrane as a result of diffusion and electro-osmosis. It is well-known that chitosan is a cationic polymer and its pK_a ranges from 6.2 to 7 thereby, in acidic solutions, it retains electrostatic properties through protonation. Although affinity of the cross-linked chitosan matrix toward water plays an important role in mass transport phenomenon of the composite structure, MMT loading and cross-linking density promotes the higher rate of proton selectivity.

To understand the methanol permeation in clay induced CS membranes, we consider that the selectivity is strongly affected by the conformational change of chitosan. The conformation change caused by the ionic and/or steric repulsion of the ionically cross-linked chitosan molecule will change the packing state of clay network and, therefore, the holes produced by the thermal motion of the chitosan molecule through which the permeant molecule diffusion will be contracted. So, the permeation of the methanol (32.04 g mol^{-1}) molecule becomes more difficult, but the permeation of the smaller hydronium (19.023 g mol^{-1}) molecule is intermittently challenged by the contraction of the holes and the selectivity increases as a result of chitosan cross-linking with the polybasic acid, H_2SO_4.[24]

A recent review on state-of-the-art advancements and factor affecting DMFC performance reiterates importance of methanol barrier property in PEMs membranes.[25] Limiting the methanol crossover in DMFCs membranes is still a widely sought after and ongoing researched topic.[26−32] Table 2 gives the some of the important membranes evaluated for their greater power density and limited methanol crossover (<90 mA/cm^2) for 1 and 2 M methanol feeds. However, at higher concentrations of methanol (4 to 10 M), measured MCCD is relatively high. In view of this, outcomes of the present study encourage the harvesting of vast natural and sustainable resources for energy applications.

CONCLUSION

In summary, natural nanocomposite chitosan-MMT membranes were prepared by an intercalation method and tested successfully with a DMFC testing station for their proton selectivity and methanol permeabilities. The XRD patterns show that the characteristic peak of Na-MMT shifted to a lower angle in the modified clay, corresponding to the formation of an intercalated-exfoliated structure. All the S-MMT intercalated and cross-linked membranes showed specific water uptake, moderate proton conductivity and reduced methanol permeability during their DMFC performances. The present study demonstrates a general strategy to convert naturally abundant materials in combination with green modification methods as a promising way to harvest high performance energy materials.

ASSOCIATED CONTENT

Supporting Information

XRD and FTIR of sulfonated MMT. This material is available free of charge via the Internet at http://pubs.acs.org.

AUTHOR INFORMATION

Corresponding Authors

*Dr. S. K. Nataraj. E-mail: sknata@gmail.com, sknataraj@csmcri.org.

*Dr. Kuei-Hsien Chen. E-mail: chenkh@pub.iams.sinica.edu.tw. Tel: +886 (02) 2366-8232. Fax: +886 (02) 2362-0200.

Notes

The authors declare no competing financial interest.

ACKNOWLEDGMENTS

This research was financially supported by Ministry of Education and National Science Council of Taiwan. Technical

DOI: 10.1021/sc5005764
ACS Sustainable Chem. Eng. 2015, 3, 302−308

support from Academia Sinica Research Project on Nano Science and Technology and is gratefully acknowledged. S.K.N. thanks DST, Government of India for INSPIRE Faculty Award (IFA12-CH-84) and Research Grant.

REFERENCES

(1) Wang, L.; Liu, Y.; Yang, X.; Fang, Y.; Chen, Y.; Wang, B. A high-performance direct methanol fuel cell with a polymer fiber membrane and RuO_2/CNTs as a cathode catalyst. *J. Mater. Chem. A* **2013**, *1*, 1834−1839.
(2) Laberty-Robert, C.; Vallé, K.; Pereira, F.; Sanchez, C. Design and properties of functional hybrid organic−inorganic membranes for fuel cells. *Chem. Soc. Rev.* **2011**, *40*, 961−1005.
(3) Rivera, H.; Lawton, J. S.; Budil, D. E.; Smotkin, E. S. The effect of sorbed methanol, current and temperature on multi-component transport in Nafion based direct methanol fuel cells. *J. Phys. Chem. B* **2008**, *112*, 8542−8548.
(4) Yamauchi, A.; Ito, T.; Yamaguchi, T. Low methanol crossover and high performance of DMFCs achieved with a pore-filling polymer electrolyte membrane. *J. Power Sources* **2007**, *174*, 170−175.
(5) Lufrano, F.; Baglio, V.; Di Blasi, O.; Staiti, P.; Antonucci, V.; Aricò, A. S. Design of efficient methanol impermeable membranes for fuel cell applications. *Phys. Chem. Chem. Phys.* **2012**, *14*, 2718−2726.
(6) Deligoz, H.; Yılmazturk, S.; Karaca, T.; Ozdemir, H.; Naci Koc, S.; Oksuzomer, F.; Durmus, A.; Ali Gurkaynak, M. Self-assembled polyelectrolyte multilayered films on Nafion with lowered methanol cross-over for DMFC applications. *J. Membr. Sci.* **2009**, *326*, 643−649.
(7) Neves, L. A.; Coelhoso, I. M.; Crespo, J. G. Methanol and gas crossover through modified Nafion membranes by incorporation of ionic liquid cations. *J. Membr. Sci.* **2010**, *360*, 363−370.
(8) Xu, C.; Zhao, T. S. In situ measurements of water crossover through the membrane for direct methanol fuel cells. *J. Power Sources* **2007**, *168*, 143−153.
(9) Tang, H. L.; Pan, M.; Jiang, S. P.; Yuan, R. Z. Modification of Nafion™ membrane to reduce methanol crossover via self-assembled Pd nanoparticles. *Mater. Lett.* **2005**, *59*, 3766−3770.
(10) Du, C. Y.; Zhao, T. S.; Yang, W. W. Effect of methanol crossover on the cathode behavior of a DMFC: A half-cell investigation. *Electrochim. Acta* **2007**, *52*, 5266−5271.
(11) Koev, S. T.; Duksstra, P. H.; Luo, X.; Rubloff, G. W.; Bentley, W. E.; Payne, G. F.; Ghodssi, R. Chitosan: An integrative biomaterial for lab-on-a-chip devices. *Lab Chip* **2010**, *10*, 3026−3042.
(12) Lui, M.; Wu, C.; Jiao, Y.; Xiong, S.; Zhou, C. Chitosan−halloysite nanotubes nanocomposite scaffolds for tissue engineering. *J. Mater. Chem. B* **2013**, *1*, 2078−2089.
(13) Valmikinathan, C. M.; Mukhatyar, V. J.; Jain, A.; Karumbaiah, L.; Dasari, M.; Bellamkonda, R. V. Photocrosslinkable chitosan based hydrogels for neural tissue engineering. *Soft Matter* **2012**, *8*, 1964−1976.
(14) Ahmed, A.; Hearn, J.; Abdelmagid, W.; Zhang, H. Dual-tuned drug release by nanofibrous scaffolds of chitosan and mesoporous silica microspheres. *J. Mater. Chem.* **2012**, *22*, 25027−25035.
(15) Jirimali, H. D.; Nagarale, R. K.; Lee, J. M.; Saravanakumar, D.; Shin, W. Chitosan-cross-linked osmium polymer composites as an efficient platform for electrochemical biosensors. *ChemPhysChem* **2013**, *14*, 2232−2236.
(16) Huanga, Y.; Cheng, C.; Tian, X.; Zheng, B.; Li, Y.; Yuan, H.; Xiao, D.; Choi, M. M. F. Low-potential amperometric detection of dopamine based on MnO_2 nanowires/chitosan modified gold electrode. *Electrochim. Acta* **2013**, *89*, 832−839.
(17) He, Z.; Liu, J.; Qiao, Y.; Li, C. M.; Tan, T. T. Y. Architecture engineering of hierarchically porous chitosan/vacuum-stripped graphene scaffold as bioanode for high performance microbial fuel cell. *Nano Lett.* **2012**, *12*, 4738−4741.
(18) Katti, K. S.; Katti, D. R.; Dash, R. Synthesis and characterization of a novel chitosan/montmorillonite/hydroxyapatite nanocomposite for bone tissue engineering. *Biomed. Mater.* **2008**, *3*, 034122−034134.
(19) Tan, W.; Zhang, Y.; Szeto, Y.-S.; Liao, L. A novel method to prepare chitosan/montmorillonite nanocomposites in the presence of hydroxy-aluminum oligomeric cations. *Compos. Sci. Technol.* **2008**, *68*, 2917−2921.
(20) Wang, C. H.; Chen, C. C.; Chen, L. C.; Shih, H. C.; Chen, K. H. Low methanol-permeable polyaniline/Nafion composite membrane for direct methanol fuel cells. *J. Power Sources* **2009**, *190*, 279−284.
(21) Du, H.-Y.; Wang, C.-H.; Hsu, H.-C.; Chang, S.-T.; Yen, S.-C.; Chen, L.-C.; Viswanathan, B.; Chen, K.-H. High performance of catalysts supported by directly grown PTFE-free micro-porous CNT layer in a proton exchange membrane fuel cell. *J. Mater. Chem.* **2011**, *21*, 2512−2516.
(22) Hofmann, E. W. M.; Kuleshova, L. N.; D'Aguanno, B. Theoretical simulations of proton conductivity: Basic principles for improving the proton conductor. *J. Power Sources* **2010**, *195*, 7743−7750.
(23) Cordova-Mateo, E.; Bertran, O.; Ferreira, C. A.; Aleman, C. Transport of hydronium ions inside poly(styrene-co-divinyl benzene) cation exchange membranes. *J. Membr. Sci.* **2013**, *428*, 393−402.
(24) Kamari, A.; Wan Ngah, W. S.; Chong, M. Y.; Cheah, M. L. Sorption of acid dyes onto GLA and H_2SO_4 cross-linked chitosan beads. *Desalination* **2009**, *249*, 1180−1189.
(25) Ahmed, M.; Dincer, I. A review on methanol crossover in direct methanol fuel cells: Challenges and achievements. *Int. J. Energy Res.* **2011**, *35*, 1213−1228.
(26) Wang, Y.; Han, G.; Tian, Z.; Wang, M.; Li, J.; Wang, X. Nafion®/SiO_2/m-BOT composite membranes for improved direct methanol fuel cell performance. *RSC Adv.* **2014**, *4*, 47129−47135.
(27) Zhu, Y.; Zieren, S.; Manthiram, A. Novel crosslinked membranes based on sulfonated poly(ether ether ketone) for direct methanol fuel cells. *Chem. Commun.* **2011**, *47*, 7410−7412.
(28) Miyake, N.; Wainright, J. S.; Savinell, R. F. *J. Electrochem. Soc.* **2001**, *148*, A905−A909.
(29) Gubler, L.; Kramer, D.; Belack, J.; Ünsal, Ö.; Schmidt, T. J.; Scherer, G.G. . *J. Electrochem. Soc.* **2007**, *154*, B981−B987.
(30) Liang, Z. X.; Zhao, T. S.; Prabhuram, J. Diphenylsilicate-incorporated Nafion® membranes for reduction of methanol crossover in direct methanol fuel cells. *J. Membr. Sci.* **2006**, *283*, 219−224.
(31) Wang, C. H.; Chen, C. C.; Chen, L. C.; Shih, H. C.; Chen, K. H. Low methanol-permeable polyaniline/Nafion composite membrane for direct methanol fuel cells. *J. Power Sources* **2009**, *190*, 279−284.
(32) Nataraj, S. K.; Wang, C.-H.; Huang, H.-C.; Du, H.-Y.; Wang, S.-F.; Chen, Y.-C.; Chen, L.-C.; Chen, K.-H. Highly proton-selective biopolymer layer-coated ion-exchange membrane for direct methanol fuel cells. *ChemSusChem* **2012**, *5*, 392−395.

DOI: 10.1021/sc5005764
ACS Sustainable Chem. Eng. 2015, 3, 302−308